Re-use of polyamide-12 in powder bed fusion and its effect on process-relevant powder characteristics and final part properties

Sanders, Benjamin; Cant, Edward; Jenkins, Michael

DOI:
10.1016/j.addma.2024.103961

Document Version
Publisher's PDF, also known as Version of record

Citation for published version (Harvard):
Sanders, B, Cant, E & Jenkins, M 2024, 'Re-use of polyamide-12 in powder bed fusion and its effect on process-relevant powder characteristics and final part properties', *Additive Manufacturing*, vol. 80, 103961. https://doi.org/10.1016/j.addma.2024.103961

Additive Manufacturing 80 (2024) 103961

Contents lists available at ScienceDirect

Additive Manufacturing

journal homepage: www.elsevier.com/locate/addma

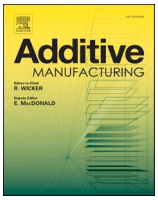

Re-use of polyamide-12 in powder bed fusion and its effect on process-relevant powder characteristics and final part properties

Benjamin Sanders [a], Edward Cant [b], Michael Jenkins [a,*]

[a] School of Metallurgy and Materials, University of Birmingham, Elms Road, Birmingham B15 2SE, UK
[b] The Manufacturing Technology Centre, Ansty Park, Coventry CV7 9JU, UK

ARTICLE INFO

Keywords:
Powder bed fusion
Polyamide-12
Powder re-use
Mechanical properties
Refresh rate

ABSTRACT

Powder bed fusion (PBF) is an additive manufacturing technique capable of fabricating highly complex, individualised, and lightweight polymer components. However, to maximise the potential of PBF, in terms of both economic efficiency and environmental sustainability, a successful powder re-use strategy is essential. During a build, ageing and degradation processes affect the re-usability of un-sintered powder, so used powder is usually refreshed with virgin material before re-use. This study considers the effectiveness of using a 70:30 refresh ratio in a specific PBF technique: laser sintering (LS). Across a total of seven printing cycles, polyamide-12 (PA-12) powder refreshed with 30 % virgin material after each build, revealed a 4.5 °C increase in melting temperature. There was also a 20 % reduction in particle flowability, which may be related to the presence of fine satellite particles and considerable particle cracking. This deterioration in powder quality resulted in a 5.8 % increase in total part porosity, and an 11 % reduction in the ultimate tensile strength of fabricated parts, over the seven build cycles. A Pearson correlation test indicated that the reduction in powder flowability was the most significant (p-value of 0.005) cause for the loss of part strength; emphasising that the revolution powder analyser could be a useful complimentary technique for determining the quality of used powder within laser sintering. Nonetheless, compared to previous studies which re-used 100 % aged PA-12 powder, without refreshing with any virgin material, the observed reduction in part strength is relatively modest. This suggests that a 70:30 refresh ratio offers a good compromise between maintaining part performance, particularly for non-critical applications, without having to add an unnecessary amount of virgin powder. Therefore, this study reveals the relationship between the deterioration of powder properties and reductions in part strength; yet highlights the benefits of operating with a 70:30 refresh ratio when re-using PA-12 powder across multiple build cycles.

1. Introduction

Laser sintering (LS) is a powder bed fusion process which has gained prominence in the additive manufacturing industry and is increasingly used for the fabrication of commercial polymer products. LS offers many benefits over more conventional techniques such as injection moulding, and other AM methods e.g., stereolithography. LS provides great design freedom, which allows the production of highly complex, individualised products [1,2]. Other advantages of LS include dimensional precision, light-weighting, and the manufacture of components with strong mechanical properties [1–6]. As a result, LS has become increasingly popular in medical (e.g., individualised prosthesis), aerospace, and architectural application areas.

In LS, thermoplastic powder, most commonly polyamide-12 (PA-12) [7–11], is stored within a build chamber at elevated temperatures. Typical LS build temperatures are between 168–172 °C [5,8], which is above the crystallisation temperature (T_c), yet just below the melting temperature (T_m), of PA-12. A CO_2 laser then provides the extra energy required to melt selected regions of the powder layer, based on the 3D-CAD data provided for the designed part. The build platform is lowered, and a fresh layer of powder is deposited before another scan causes polymer particles to fuse together, in the desired shape for that 2D cross-section [3,4]. This is repeated until all the necessary powder coalesces, layer-by-layer, to form a 3D part [1,5,12,13]. During the LS process, the build chamber utilises an inert gas environment to restrict oxidative degradation [14], however many state of the art LS machines still contain 2–5 % residual oxygen [8,15]. Within LS, PA-12 dominates the market for polymeric feedstock materials due to its wide processing

* Corresponding author.
E-mail address: m.j.jenkins@bham.ac.uk (M. Jenkins).

https://doi.org/10.1016/j.addma.2024.103961
Received 8 June 2023; Received in revised form 22 November 2023; Accepted 3 January 2024
Available online 6 January 2024

window, whereby there is a large temperature range between the start of melting and the start of crystallisation. This helps maximise powder consolidation and limit part warpage [6,16,17]. PA-12 powder also displays good flowability, relatively low moisture absorption, and a high sintering rate [6,8,16,18].

Another significant advantage of LS is that the sintered and consolidated particles are contained within an unfused powder bed, so the removal of support structures is not required [1,3,19,20]. Unconnected islands and overhangs are supported by the surrounding, un-sintered powder within the build chamber [1,19]. As a result, the most complex features can be manufactured and multiple parts, of different sizes and geometries, can be arranged together, without restrictions, within the powder bed. This enhances part nesting and increases productivity [1–4,20]. On the other hand, as the majority of powder within a build chamber is used as support material, LS has an inefficient powder utilisation rate and, for each build, only ~10–20 % of the powder deposited is consolidated into final parts [4,21–24]. Therefore, the remaining 80–90 % of un-sintered powder must be re-used to ensure the process is financially feasible and environmentally sustainable [3,4,10].

LS-grade PA-12 powder is estimated to be 5000 % more expensive, per kg, than equivalent polyamide feedstock for injection moulding [25]. Therefore, maximising powder re-use is economically vital [3,10,23,25]. However, during a build cycle, PA-12 powder is exposed to high temperatures for extended periods of time. This inevitably results in ageing and degradation processes which limit the re-usability of the material [2–4,8–10,24,26]. LS also involves a cooling stage, which is often double the duration of the build, prolonging ageing of the un-sintered powder [3,4,27]. Ageing and degradation processes possess the capability to alter the intrinsic and extrinsic properties of PA-12 powder; following multiple refreshing cycles the feedstock material may display heterogeneous behaviour, with a wide variation in properties [17]. This is problematic because, to ensure the fabrication of high-quality parts, LS must follow stringent processing conditions and requires extremely close control of material properties [25,28]. Key intrinsic parameters include thermal properties such as the processing window, T_m, and development of crystallinity. Whilst particle morphology (e.g., sphericity, shape, and size), and particle flowability are crucial extrinsic characteristics that are imperative to the successful production of LS parts [25,28]. As such, ageing processes may limit the re-usability and processability of PA-12 powder, which could ultimately result in the manufacture of underperforming LS components. Therefore, it is common practice for virgin PA-12 powder to be added to the un-sintered, “used” powder, in an attempt to restore the material properties. This refreshed blend is then used in subsequent builds. The refresh ratio defines the ratio of used to virgin material, and commonly 50–70 % of used powder is recycled for future use, although the exact refresh rate differs from supplier to supplier [2–4,10,24]. Nevertheless, many operators continue to exclusively use a 50:50 refresh ratio, in an attempt to maximise part quality. However, refreshing with 50 % virgin powder often results in relatively un-aged powder being discarded unnecessarily, so this recycling strategy can be inefficient and wasteful. In order to improve powder recycling, a compromise between maximising powder re-use, without causing a significant reduction in powder and final part quality is required.

Ageing and degradation of PA-12 powder within LS is a complex problem. At the typical powder bed temperature of ~170 °C, there is an interplay between various chemical ageing processes as they often occur simultaneously [14,29]. Solid-state polycondensation (post-condensation) of un-sintered PA-12 powder involves lengthening of polymer chains through reactions of end groups; this linear chain growth leads to an increase in molecular weight (M_w) [10,11,23,26,30]. On the other hand, chain scission and cross-linking, which usually have opposing effects, can occur as a result of thermo-oxidation [2,8,23]. Most LS machines utilise an inert (or low oxygen) environment in an attempt to limit the effects of thermo-oxidation. Nonetheless, laser radiation can locally form hydrogen molecule radicals [15,31]. With extended time, these free radicals can combine with the unavoidable, residual oxygen remaining in the build chamber and initiate oxidation [15]. Furthermore, when semi-crystalline polymers are heated to higher temperatures, there is increased chain mobility in the amorphous regions which may allow developments in crystallinity via a secondary crystallisation process, such as lamella thickening [32–35]. Previous studies have suggested that polycondensation is the dominant ageing phenomena within LS [8,11,22,23,36–39], however, the possibility of other processes occurring with repeated powder re-use cannot be ignored.

The effect of ageing on the re-usability of PA-12 powder within LS has previously been explored from a range of perspectives. Multiple papers have attempted to simulate the conditions found within a LS build chamber by storing PA-12 powder at various temperatures, for a range of time periods, within a nitrogen flushed or vacuum oven [4,12,14,22,40]. These authors used a range of techniques such as differential scanning calorimetry (DSC), scanning electron microscopy (SEM), and size exclusion chromatography (SEC) to investigate the change in powder properties as a result of ageing. Although useful for improving the understanding of ageing and degradation, oven conditions cannot be directly compared to a LS build process, nor reveal the effect ageing has on the mechanical properties of LS parts. Other studies have focussed specifically on the effect of oven conditioning, or powder re-use within LS, on the change in melt viscosity of PA-12 powder, often using melt flow rate (MFR) as the primary measurement [2,3,10,40,41]. Generally, they reported that, with increased ageing of PA-12 powder, MFR significantly reduced, indicating an increase in melt viscosity. This correlates to an increase in molecular weight (M_w), which was attributed to polycondensation. However, exclusively using MFR to characterise a change in powder properties has limitations, as it is an energy-intensive technique and only concentrates on one material property. Consequently, MFR is unable to detect other types of ageing, such as secondary crystallisation; it also fails to account for more process-relevant parameters, such as particle morphology and flowability, which likely have a significant effect on the property profile of laser sintered parts.

Furthermore, some papers compared virgin, aged, and once-recycled powder samples by characterising the change in T_m, coalescence behaviour, particle flowability, and M_w as a result of ageing [8,9,11,42]. Zarringhalam et al., re-used PA-12 powder with a 67:33 refresh rate and observed a 143 % increase in M_w after just one build cycle [9]. Conversely, using a 50:50 refresh ratio, Sillani et al., saw a 170 % increase in M_w[11]. Comparing these two papers suggests that the extent of polycondensation, and subsequent increases in M_w, is greater within the study that refreshed with more virgin powder. Although there may have been slight differences in the specific build processing parameters between these two investigations, which could have altered the rate of polycondensation, these results indicate that using higher refresh rates may not always be beneficial for controlling the properties of feedstock powder. This one example provides some insight into the inefficiency of current powder re-use strategies, such as exclusively using a 50:50 refresh ratio. Nevertheless, despite providing valuable insight into the change in powder behaviour across one build cycle, further investigation is required to determine the effect on powder and part properties across multiple build cycles. This is necessary because, within industry, it is essential that powder is re-used for multiple cycles, particularly when aiming to minimise environmental impact and cost.

Multiple papers have begun to explore the effect of ageing when re-using PA-12 powder across multiple build cycles, without refreshing with virgin material [16–18,23,26,37,43]. They reported that with increased PA-12 powder re-use, there is an increase in melt viscosity [23,26,37,43] which ultimately contributes to reductions in part density and part strength [26,37,43]. However, these studies either don’t reveal build times, so the total cumulative build time is unknown [37,43,44], or use build times much shorter than what is common within industry [23,26]. As such, the cumulative build times, even across five process cycles, remain relatively modest (e.g., < 27 h [23]) and the extent of

material ageing is limited. More recently Alo et al., exposed PA-12 powder to eight build cycles and, with increased cumulative build time, observed a significant decrease in the degree of crystallinity, as well as a change in the size and shape distribution of feedstock powder. This change in powder properties resulted in significant reductions in the strength of sintered parts [16,17]. However, it is important to highlight that, in between build cycles the feedstock material was not refreshed with virgin powder, which contradicts common industrial practice. As such, there is limited understanding regarding the effect of refreshing used powder with virgin material, when re-using PA-12 powder across an extended number of LS cycles, with a large cumulative build time. Determining whether virgin refresh rates are able to counteract the changes in used powder properties, as a result of ageing, is crucial to help predict the property profile of LS parts. Current industry practices generally use either 50:50 or 70:30 refresh ratios. In this work a 30 % refresh rate was implemented in order to investigate the possibility of re-using more powder, without compromising final part performance.

Therefore, this study intends to quantify the effect of ageing on the relationship between process-relevant properties of PA-12 powder, and the behaviour of LS parts, when operating with a 70:30 refresh ratio. PA-12 feedstock, refreshed with 30 % virgin powder before each build, was exposed to seven LS cycles, with an extended cumulative build time of over 200 h, including the cool-down. This work provides quantitative data about the capability of a 30 % refresh ratio for restoring the properties of used powder, and ultimately determines whether a 70:30 refresh ratio offers a good compromise between increasing powder re-use, without a detriment to final part quality. In addition, the most suitable characterisation techniques for determining PA-12 powder quality were identified, providing more information about the suitability of un-sintered powder for re-use within LS. This will help inform more efficient classification of used powder recovered from different build cycles, thereby helping the industry realise improved recycling strategies.

2. Experimental methodology

2.1. Materials and sample preparation

An outline of the sample preparation procedure is shown in Fig. 1. The work was carried out using industrial grade PA-12 powder (PA2200, EOS GmbH), whilst laser sintered parts were fabricated using standard EOS build parameters [45], so print conditions were 'locked-in'. For each build, the chamber temperature was 170 ± 1 °C, and the unloading temperature was 130 ± 1 °C. PA-12 powder was re-used for a total of seven build cycles, using a refresh ratio of 70:30 (used: virgin). Therefore, as the supplied powder is refreshed before each build, only ~12 % of 'used' powder recovered from build 7 would have been through every build cycle. To quantify the time that refreshed powder was exposed to the processing temperature, and to better indicate the extent of powder ageing, the cumulative build time (t_c) was also recorded. After seven builds, the t_c was 98 h, whilst the total cumulative time (including the cool down) was 208 h. The approximate cooldown time, of build to breakout temperature, ranged from 14 to 18 h across the seven build cycles.

During each build the refreshed powder was used to produce tensile samples in 3 different build orientations (XY, ZX and YX 45 degree), as shown in Fig. 2. The LS dog-bone tensile specimens had a gauge length of 70 mm, width 12.89 mm and thickness of ~3 mm, whereby a micrometre screw gauge was used to measure the sample thickness.

2.2. Powder characterisation

Differential scanning calorimetry (DSC) analysis of virgin, used, and

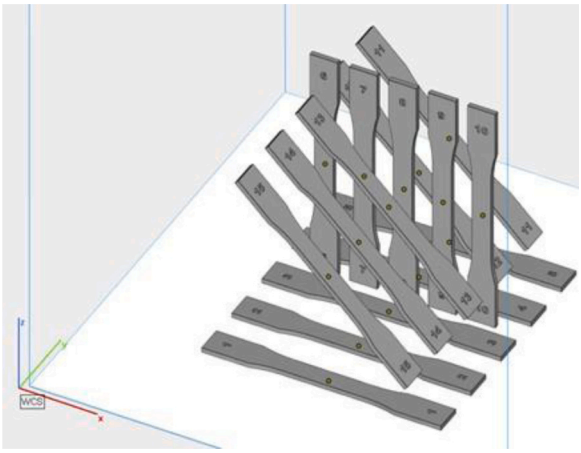

Fig. 2. Build orientations of tensile samples. 1–5 are horizontal orientation (XY), 6–10 are vertical orientation (ZX) and 11–15 have an angular orientation (YX 45 degree).

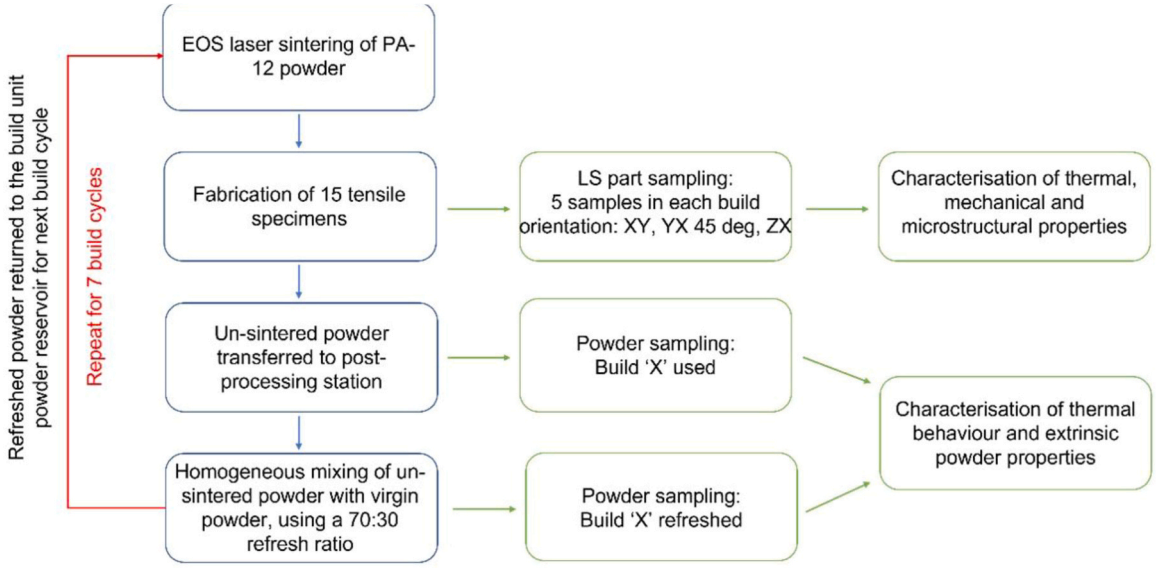

Fig. 1. Summary of the work package, sampling procedure and sample characterisation.

refreshed powder was performed using a Mettler Toledo DSC-1. Before conducting material characterisation experiments, the DSC was calibrated using zinc (T_m 419.5 °C, ΔH_f 107.5 Jg^{-1}) and indium (T_m 156.6 °C, ΔH_f 28.45 Jg^{-1}); nitrogen gas (flow rate 100 $mLmin^{-1}$) was used to limit oxidative degradation occurring during experiments. Samples, with a mass of 6 ± 0.5 mg, were heated from 25–220 °C, using a heating rate of 10 $degreeCmin^{-1}$ and then cooled at the same rate. Analysis was primarily carried out on the first heating and cooling cycle, to understand the effect of the LS build conditions on the thermal properties of PA-12 powder. Integration of the endothermic melting peak provides a value for heat of fusion (ΔH_f). This can be used to estimate percentage crystallinity (X_c) using Eq. 1, whereby $\Delta H_f = 209.3 Jg^{-1}$ (100 % crystalline PA-12) [11]. For every sample, 3 DSC repeats were conducted, and an average calculated.

$$X_c \quad (\%) = \frac{\Delta H_f}{\Delta H_f{}^0} \quad X100 \tag{1}$$

Various process-relevant, extrinsic powder properties were also analysed for virgin, used, and refreshed powder samples. A Mercury Scientific revolution powder analyser (RPA) quantified particle flowability. A low RPM was used so that the flowability of powder particles could be measured by analysing a sequence of avalanches. Full experimental parameters are outlined in Table 1. For each batch of PA-12 powder, 3 repeats were recorded, and an average taken. The change in particle size distribution (PSD), with build number, was evaluated using a Malvern Mastersizer 2000 which uses laser diffraction to determine the particle size of PA-12 powder suspended in water. Tests were conducted according to the ASTM B822–10 standard test method for PSD of powders and compounds. Powder particle shape and microstructure was characterised using scanning electron microscopy (SEM). To prepare the sample a single layer of PA-12 powder was applied onto carbon adhesive, on an aluminium stub. Samples were sputter coated in gold using an Enscope Engineering LTD. SC500 gold sputter coater to reduce surface charging in the samples. To ensure the polymer sample was conductive, copper tape was applied from the aluminium stub to the powder surface. The sample was viewed using a tabletop Hitachi 3030+ SEM, under vacuum, with a voltage of 15 kW and using a mix of backscattered electrons (BSE) and secondary electrons (SE) signals. Magnifications ranged from 40x to 500x, depending on the feature of interest, and the auto-focus/auto-contrast functions were utilised. This was repeated with each batch of refreshed PA-12 powder.

2.3. LS part characterisation

The thermal behaviour of LS parts was characterised using the same DSC method described in *Section 2.2* . DSC samples, with a mass of 10 ± 0.5 mg, were prepared by punching discs from the grip sections of tensile specimens.

To establish the influence of powder re-use on the mechanical properties of LS parts, all tensile samples were examined on an Instron 7877 material tester. Each experiment was run according to ASTM D638 tensile tension testing for plastics, with a 20 kN load cell and strain rate of 10 mm/min. Bluehill universal materials analysis software (Instron) provided measurements of ultimate tensile strength (UTS), yield strength (YS), and elongation at break (EAB). The Young's modulus was estimated from the linear elastic region of the stress-strain curves. For each build number, in every build orientation, an average was taken from 5 samples. The statistical significance of the data was measured using MANOVA analysis and post-hoc T-tests, with the Bonferroni correction, to indicate which build number showed significant changes in mechanical properties.

Following mechanical testing, samples were further characterised using SEM. The fracture surface of randomly selected tensile specimens, from each build number, were prepared and viewed using the same method described in *Section 2.2* . To quantify the change in porosity of LS tensile specimens with increased build number, multiple samples were analysed using x-ray computed topography (XCT). The scans were performed using a Diondo D2 micro-CT machine using a voltage of 30 kV, a current of 200μA, and 2500 projections. The magnification was x17.3, which yields a sufficient voxel size to accurately measure porosity. Pore size, number, and overall percentage porosity were estimated using ImageJ software.

Table 1
RPA flowability test set up parameters. Experiments were conducted under a room temperature of 25 °C, and room humidity of 40 %.

Parameter	Value
Sample Volume	25 cc (tap density)
Rotating speed	0.3 RPM
Preparation time	60 s
Avalanche threshold	0-65 %
Angle calculation	Half
No. of avalanches recorded	150
Image capturing rate	25 frames per second

3. Results and discussion

3.1. Powder characterisation

3.1.1. Thermal behaviour

The change in the melting behaviour of used and refreshed powder, across a total of seven build cycles, was measured using DSC (Fig. 3). With increased powder re-use, used powder displayed a gradual increase in peak melting temperature (T_m) and endpoint of melting ($T_m e$), which is particularly important for subsequent LS builds. Conversely, the refreshed powder shows an initial increase in T_m, but then any further change is less significant.

The difference in the melting behaviour of used and refreshed powder, across multiple build cycles, is shown more clearly in Fig. 4. The average peak T_m of used PA-12 powder increases almost linearly until build 5, at which point T_m is 4.2 °C greater than virgin material. This is followed by a 0.5 °C reduction in T_m; within the sensitivity of the DSC, this change is considered insignificant, nevertheless it represents a change in the observed trend. On the other hand, refreshed powder also shows an initial rise in T_m and by build 2, refreshed powder has a peak T_m 3.4 °C higher than virgin material. However, the increase then plateaus and there is no further change until build 6, where a 1 °C rise is observed (Fig. 4a).

In both used and refreshed powder, the increase in T_m may be explained by solid-state polycondensation, as reported previously [22,29,37,38,42]. Prior research revealed reservations about how a process which occurs primarily in the amorphous phase can significantly affect the melting of crystalline structures [35]. Nonetheless, it is widely reported that the inert (or low oxygen) conditions found within a LS build chamber favours the polycondensation reaction, which increases the rate of macromolecular chain growth [8,11,22,23,36–39]. This can lead to an increased molecular weight, resulting in a higher melting point [23,24,29]. Increases in T_m could also be attributed to cross-linking [29,37], but cross-links usually form as a product of the thermo-oxidation cycle [46–48], so is unlikely to occur in a LS build chamber with limited oxygen. However, secondary crystallisation, an ageing process often overlooked in previous LS studies, can also contribute to changes in the melting behaviour [23,24,29,47,49]. At the elevated temperatures found within an LS build chamber, amorphous chains have greater mobility, which can allow further crystallinity to develop via a continuous lamellar thickening process, resulting in an increased T_m [35]. The DSC was unable to identify a significant increase in sample crystallinity (Table 2), but this characterisation technique may not be sensitive enough to detect the gradual lamellar thickening process. Therefore, secondary crystallisation occurring within unfused PA-12 powder cannot be ruled out, and lamellar thickening may contribute to an increased T_m, in addition to the polycondensation process.

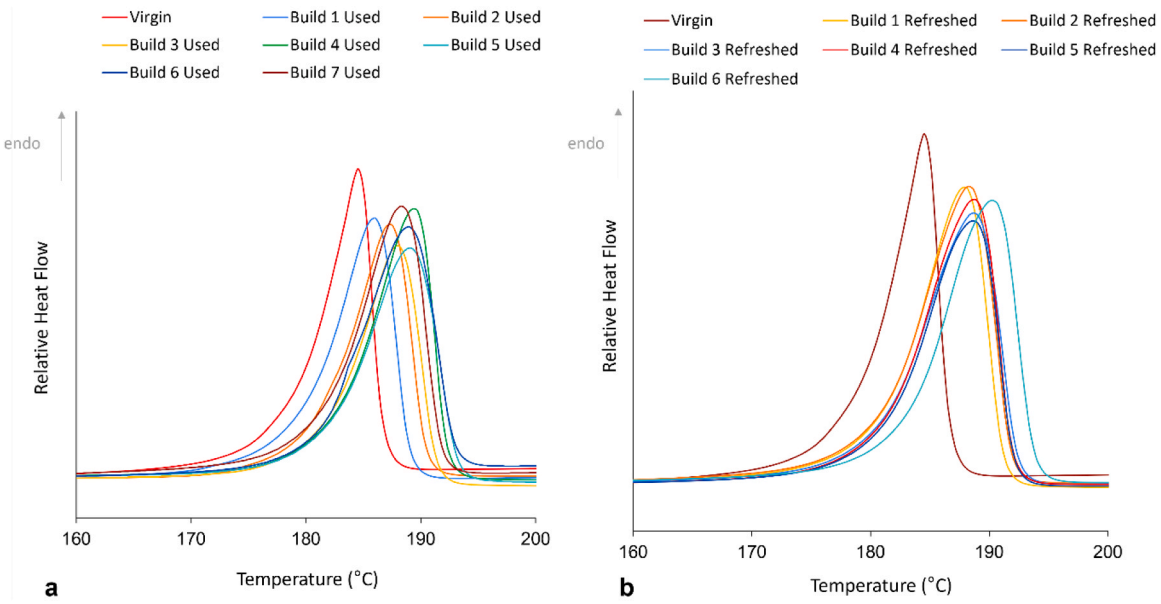

Fig. 3. The change in melting behaviour of a) used powder and b) refreshed powder, with increased build number.

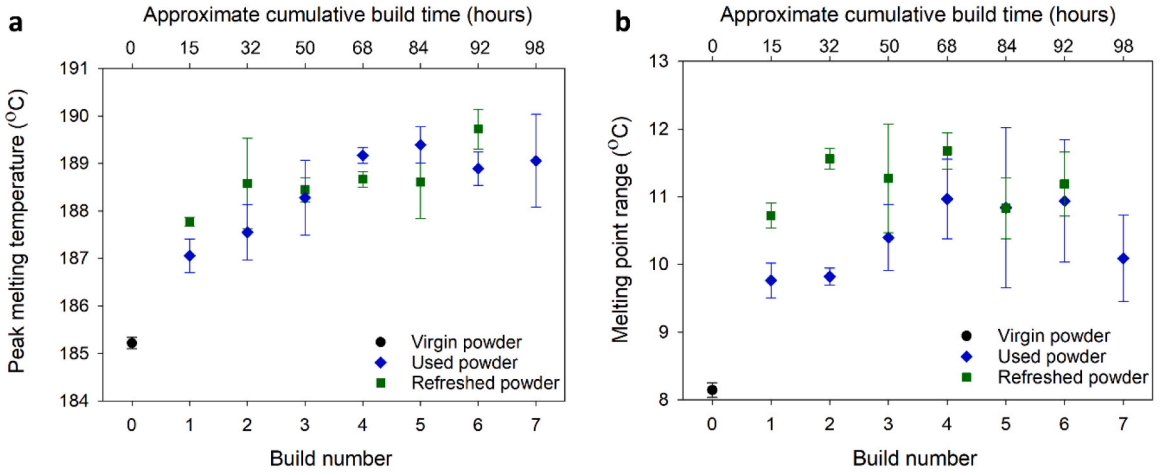

Fig. 4. Comparing the average change in a) Peak T_m and b) T_m range for used and refreshed PA-12 powder across 7 LS build cycles and as a function of t_c. All datapoints are taken as an average from 3 repeats.

Table 2
The change in thermal properties of used and refreshed powder, as a function of build number, measured via DSC.

Used powder					*Refreshed powder*			
Build number	**Peak T_m (°C)**	**Endpoint T_m (°C)**	**Peak T_c (°C)**	**Crystallinity (%)**	**Peak T_m (°C)**	**Endpoint T_m (°C)**	**Peak T_c (°C)**	**Crystallinity (%)**
Virgin	185.2 (± 0.12)	187.7 (± 1.90)	145.8 (± 0.77)	47 (± 3.8)	185.2 (± 0.12)	187.7 (± 1.90)	145.8 (± 0.77)	47 (± 3.8)
1	187.1 (± 0.35)	190.1 (± 1.22)	144.0 (± 0.88)	47 (± 0.8)	187.8 (± 0.09)	191.1 (± 0.24))	146.0 (± 0.00)	51 (± 0.7)
2	187.6 (± 0.59)	190.5 (± 1.09)	143.9 (± 0.70)	49 (± 4.2)	188.6 (± 0.95)	192.1 (± 1.15)	145.7 (± 0.96)	50 (± 1.9)
3	188.3 (± 0.79)	191.8 (± 1.31)	143.2 (± 1.02)	48 (± 2.0)	188.4 (± 0.25)	191.7 (± 0.69)	145.7 (± 0.00)	48 (± 1.8)
4	189.2 (± 0.17)	192.8 (± 0.41)	144.4 (± 0.20)	49 (± 1.0)	188.7 (± 0.17)	192.3 (± 0.19)	145.8 (± 0.19)	48 (± 0.8)
5	189.4 (± 0.38)	193.0 (± 0.23)	144.8 (± 0.19)	50 (± 0.5)	188.6 (± 0.77)	191.9 (± 0.84)	146.0 (± 0.88)	49 (± 1.0)
6	188.9 (± 0.35)	192.2 (± 0.71)	144.7 (± 0.00)	48 (± 1.7)	189.7 (± 0.42)	193.1 (± 0.35)	144.7 (± 0.33)	50 (± 1.1)
7	189.1 (± 0.98)	192.1 (± 0.74)	144.8 (± 0.69)	49 (± 1.0)	-	-	-	-

In refreshed powder, virgin material is added in an attempt to try and restore powder properties; the aim is to prevent further increases in T_m and return the thermal properties back towards that of the virgin powder. However, in this work over the first two build cycles, the increase in T_m of refreshed powder is slightly greater than the change in used samples. Measuring the peak melting temperature of polymers within the DSC is only accurate to ± 0.5 °C, so the initial variability between used and refreshed samples is not considered significant. Nonetheless, it does indicate that a 30 % refresh ratio may not be high enough to completely overcome the effects of polycondensation and secondary crystallisation. As a result, over the first two build cycles, refreshed powder still shows a significant increase in melting temperature. This could be explained by previous suggestions that polycondensation occurs primarily on thermally unstressed (virgin) powder, whilst the rate of chain growth within used, aged powder is lowered due to the reduced availability of end-groups [2,10,29]. Fig. 4a shows that the major increase in T_m occurs during build 1, where 100 % of material is thermally "unstressed". Following build 2, 50 % of the powder has been used within two full build cycles, so the rate of polycondensation may reduce and refreshing with virgin powder now prevents further changes in the melting temperature. This is supported by the behaviour of used powder samples. Between virgin material to used powder recovered from build 1, the increase in T_m has a gradient of 1.8, whilst the gradient for the increase over builds 2 to 5 is 0.6, emphasising that the major change occurs on thermally unstressed material. In the used samples, no virgin material is added so T_m continues to increase, albeit at a reduced rate. On the other hand, the plateau observed in the refreshed samples after build 2 emphasises that the refresh rate is now successful in inhibiting further changes in T_m.

Used and refreshed powder samples also show increases in melting point range, as a function of powder re-use, and at each build number the T_m range for the refreshed mixture is slightly greater than used powder (Fig. 4b). The difference between used and refreshed powder makes sense because, when 30 % virgin powder is added to the used material, the refreshed blend now contains two separate populations; virgin powder particles which should melt at lower temperatures, and used powder particles that are expected to have a higher T_m. As a result, there is a change in shape and broadening of the endothermic melting peak. A rise in the endpoint of melting, as shown in Table 2, will also contribute to the increase in T_m range; this explains why there is a broadening of the melting interval within both used and refreshed samples, as a function of build number. Analogous to the changes in peak T_m, the most significant increase in T_m range occurs over the first two build cycles. Furthermore, in both types of powder, the thermal properties appear to become more heterogeneous with increased build number, demonstrated by rising standard deviation values. In the context of LS, increases in the endpoint of melting are important because it means that more energy is required for complete melting of powder particles. So, assuming that build processing parameters remain constant, this could lead to incomplete particle melting and an increased number of nascent particles, which hinders particle coalescence during sintering, resulting in greater pore density [8,15,24,26]. The industrial significance of the observed variations in melting temperature, as a function of build number, can be further understood upon characterisation of the behaviour of final LS parts (Section 3.2.2).

Increased powder re-use across multiple LS build cycles also influences the crystallisation behaviour of PA-12 on cooling from the melt (Table 2). Although the change in crystallisation temperature (T_c), with build number, doesn't follow the same trend as the melting behaviour, there is a similar difference between used and refreshed powder. In the used material there is an immediate reduction in T_c and used powder recovered from build 3 has a T_c 2.6 °C lower than virgin material. Reductions in T_c provide further evidence of solid-state polycondensation occurring within un-sintered powder during LS builds. Lengthening of polymer chains via polycondensation leads to a greater number of entanglements, which hinders chain ordering and postpones the crystallisation process [3,4,8,9,14,23]. Following build 3, there is no further change in T_c of used powder, which further supports the suggestion that the rate of the chain growth decreases within aged powder, due to a reduced availability of active end groups [2,10,29].

In refreshed powder, the only significant change in crystallisation behaviour occurs after 5 build cycles, at which point there is a 1.5 °C reduction in T_c, mirroring the 1.1 °C increase in T_m observed at the same build number. At this point, a higher volume of powder has been re-used in multiple build cycles, so one might expect the recovered material to be more degraded. The change in trend following build 5 indicates the point at which a refresh ratio of 70:30 may be insufficient to restore the thermal properties of PA-12 powder. Providing that there is close monitoring of powder quality after each build, there is potential for industry to extend powder re-usability. Small modifications of the processing parameters (e.g., laser power and scanning speed) at the stage where it appears the thermal properties can no longer be restored, could help ensure that the powder is still suitable for re-use in subsequent builds. However, it should be recognised that altering processing parameters may then alter the rate of degradation processes. Alternatively, for industrial applications where the control of thermal properties is especially crucial, the use of flexible refresh ratios could be explored. For example, over the first two build cycles, where the rate of polycondensation is heightened, a greater proportion of virgin powder could be added to try and prevent the observed increases in melting temperature. A similar approach could also be taken following further changes in thermal properties after build 5. However, the use of different refresh ratios was beyond the scope of this project; further work would be required to investigate the effectiveness of higher virgin refresh rates.

3.1.2. *Extrinsic powder properties*

The re-usability of PA-12 powder across multiple LS builds is heavily dependent on various material properties [25,28]. In this section, analysis has been focused on 'refreshed' samples because this was the powder reintroduced into the bed chamber before each build, and the material that final LS components were fabricated from. Within industry, the importance of utilising a more modern powder characterisation methodology, which provides understanding of the material properties required to fabricate high quality parts consistently, has been recognised in recent years [25,50]. As such, there is currently a growing demand for a more equivalent analysis method to determine flowability in LS systems [50]. Powder flowability is closely related with spreadability, which is required within LS to ensure a uniform layer thickness, smooth even surfaces, and equal particle size distribution across a powder bed. This ensures homogeneous powder layers and subsequently consistent properties of LS parts. The revolution powder analyser (RPA) is a particularly useful characterisation technique because it can measure the flowability of powder particles under a similar stress state to when powder is spread over the build platform during LS. Although the RPA is not a direct representation of what occurs during LS with regards to the re-coater blade, it provides more process relevant data than other, more commonly used characterisation techniques, such as melt flow rate. The RPA exports high volumes of data, however the key characterisation indexes regarding particle flowability are avalanche angle (a_a), avalanche time (a_t), and avalanche energy (a_e) [11,50,51], so these parameters are the focus of this study. With increased build number there is an increase in the median a_a and a_a distribution, both of which indicate a reduction in flowability of refreshed powder (Fig. 5a). This was supported by a MANOVA analysis, which emphasised that there was a statistically significant difference in a_a as a function of build number (Fig. 5b). The change in a_a follows an almost identical trend to the melting behaviour of refreshed powder, which increases confidence in the significance of these results. Across the first two builds there was a 12.2 % increase in a_a, this was followed by a plateau, before another 7 % increase following build 6. Post-hoc t-tests, with the Bonferroni correction, emphasised that, the powder recovered from build 2 showed a statistically significant difference to virgin powder, as denoted by * in

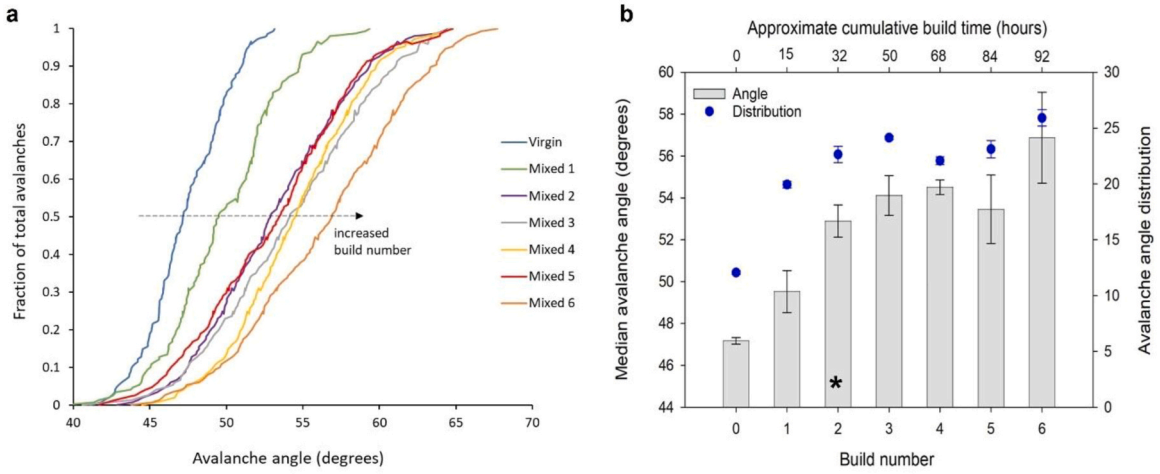

Fig. 5. Displays the change in a) cumulative avalanche angle and b) average avalanche angle / average avalanche angle distribution, as a function of build number and t_c. All datapoints in a) and b) are taken as an average of 3 repeats.

Fig. 5b.

Avalanche energy and avalanche time showed similar behaviour to the observed increase in avalanche angle (Table 3). These changes emphasise that, with increased powder re-use, there was a reduction in powder flowability. This may have consequences for subsequent LS builds because when using powder with reduced particle flow, it may hinder how easily powder can be spread across the build platform. Therefore, powder may not be uniformly distributed, and during sintering this could result in the fabrication of parts with decreased density, increased porosity, and significant layer delamination [8,26,52]. These factors have the potential to decrease the mechanical properties and aesthetics (e.g., orange peel) of parts, which may render the component un-suitable for use in its industrial application.

Reductions in particle flowability have previously been associated with changes in particle size [8,26,28,52]. LS polymer powders require a particle size distribution between 20 μm and 80 μm; fine particles that are too small induce stickiness whilst larger particles hinder the flowability of the powder across the powder bed [28]. Some authors have reported a broadening of the polydispersity index (PDI) in used powder, which indicates the presence of large molecules [22,29,49]. These large particles may form in aged powder due to severe agglomeration as a result of greater cohesive forces between particles [15,17]. Particle size analysis was carried out to try and understand whether the reductions in powder flowability were caused by a significant change in particle size. However, with increasing build number the Malvern mastersizer was unable to detect any change in particle size distribution (Table 4). Therefore, although there is evidence of polycondensation occurring (Section 3.1.1), it does not appear to cause agglomeration of particles, or an increase in particle size, so may not explain the reduction in powder flow observed in this study.

Changes in particle sphericity and surface smoothness can also affect the flowability of PA-12 powder. Perfectly spherical particles, with a smooth surface, allow adjacent particles to move freely past each other, which reduces friction and mechanical interlocking during re-coater spreading [17]. Smooth and spherical powder also assists powder flow, minimises agglomeration, and enables greater packing densities [8,53]. Nonetheless, despite particle sphericity being highly beneficial for LS processing, most commercial PA-12 powders are produced via precipitation from solvents, such as ethanol, and forming fully spherical particles using this method can be difficult [54–56]. Samples of virgin and refreshed PA-12 powder were analysed using SEM to monitor whether there was a change in particle morphology with build number. Virgin powder contained particles with a relatively spherical shape and fairly smooth surface, whilst there was limited particle cracking (Fig. 6a). In contrast, the powder recovered from build 3, showed a greater number of non-spherical particles, with many displaying a more elongated, oval shape (Fig. 6b), as observed in previous studies [17,18,56].

Nevertheless, the more significant change in particle morphology is the considerable increase in particle cracking and the appearance of "satellite" particles which attach themselves to larger particles; it is likely these fine fragments cannot be detected by the Malvern Mastersizer as they are not considered as independent particles. Powder recovered from build 3 showed some evidence of particle cracking (Fig. 7a), but, the extent of cracking is accentuated in powder recovered from build 6 (Fig. 7b). Similarly, within virgin powder some fine satellite particles are present (Fig. 6), however they significantly increase in number within samples which have been recovered after use in multiple LS builds (Fig. 7). In powder recovered from build 6, fragmented, satellite particles are widespread and appear to cluster around crack regions within bigger particles. Satellite particles are thought to form as a result of the high temperatures present within a LS build chamber which makes finer particles stick to the surface of larger particles [17].

It should be noted that the presence of irregular particle shapes and particle cracking can still exist in virgin powder, but to a much lesser

Table 3
Average change in the key markers of refreshed powder particle flowability, with build number, measured using the revolution particle analyser.

Build Number	Avalanche angle (degrees)	Avalanche energy (mJ)	Avalanche time (seconds)
0	47.2 ± 0.16	11.5 ± 0.73	4.1 ± 0.42
1	49.5 ± 0.97	12.6 ± 1.20	4.7 ± 0.62
2	52.9 ± 0.85	12.9 ± 1.30	4.9 ± 0.45
3	54.1 ± 0.91	12.7 ± 1.12	5.0 ± 0.46
4	54.5 ± 0.92	13.1 ± 1.18	5.1 ± 0.05
5	53.5 ± 0.61	13.5 ± 0.73	5.1 ± 0.49
6	56.87 ± 0.88	14.7 ± 0.94	5.4 ± 0.25

Table 4
Particle size distribution analysis of refreshed powder at each build number.

Build number	Dx10	Dx50	Dx90
0	37.0 ± 0.90	56.8 ± 0.50	85.0 ± 0.70
1	37.2 ± 0.78	56.9 ± 0.45	84.8 ± 0.46
2	36.8 ± 0.72	56.4 ± 0.64	84.5 ± 0.38
3	37.0 ± 1.42	56.2 ± 0.87	83.5 ± 0.72
4	37.1 ± 0.20	56.5 ± 0.31	84.9 ± 0.40
5	33.9 ± 1.67	54.8 ± 0.60	84.4 ± 0.66
6	36.0 ± 0.72	55.0 ± 0.35	84.5 ± 0.35

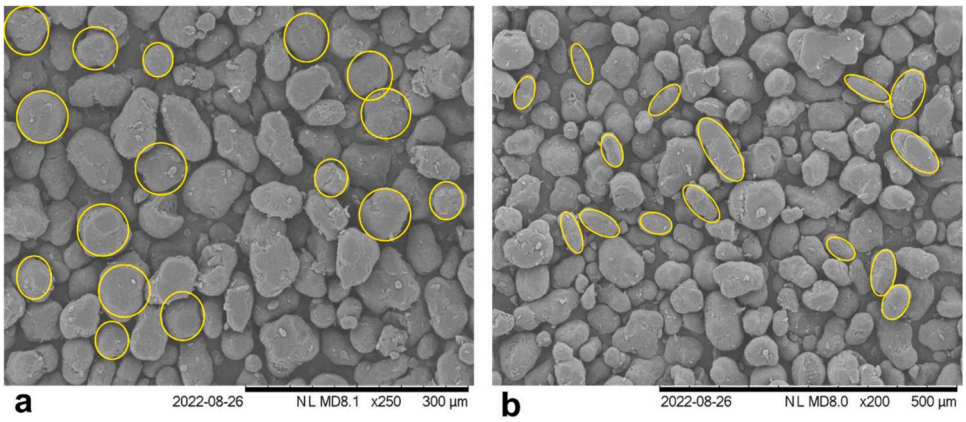

Fig. 6. SEM images of showing particle morphology of a) virgin powder and b) refreshed powder recovered from build 3.

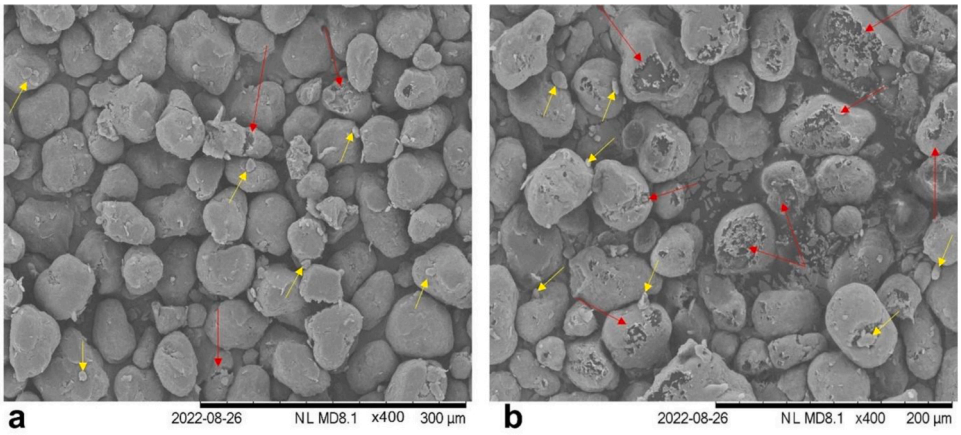

Fig. 7. SEM images displaying evidence of significant particle cracking (red arrows) and presence of "satellite particles" (yellow arrows) in a) refreshed powder recovered from build 3, and more significantly in b) refreshed powder revered from build 6.

extent. As such, these results indicate that with increased powder re-use there is a deterioration of particle structure and a reduction in surface smoothness, which can be explained by a variety of factors. Evaporation of the ethanol solvent used in powder processing, or moisture remaining in the material, may explain the formation of particle cracks [8]. With increased time spent at the elevated temperatures found within a LS build chamber, evaporation will likely occur to a greater extent, so could contribute to the deterioration of powder structure. Equally, if powder handling between build cycles is not conducted in a controlled environment, this may allow more moisture to diffuse into the powder, resulting in further evaporation in subsequent builds. Additionally, successive re-use in multiple builds exposes powder to repeated expansion and shrinkage cycles, which may also cause increased cracking and particle fragmentation [17,57]. Similarly, deterioration of the particle surface could be related to a mechanical interaction with the re-coater blade.

The observed changes in powder morphology likely explains the reduction in particle flowability, and this could weaken the mechanical properties of sintered parts [26,52]. Furthermore, particle cracking may impair the surface finish of parts, resulting in an 'orange peel' appearance, which has been commonly reported when parts are fabricated using severely degraded powder [3,4,8,23,24,37].

3.2. LS part characterisation

Analysis of the physical and mechanical properties of LS parts provides more information about the relationship between the deterioration of powder properties and the reduced quality of final parts. This delivers increased understanding of the extent of quality compromise over multiple build cycles, when operating with a 70:30 refresh ratio; demonstrating how much performance is lost with increased, extended powder re-use.

3.2.1. Part microstructure

3.2.1.1. Differential scanning calorimetry (DSC). The thermal behaviour of sintered parts was characterised using DSC (Fig. 8). Parts fabricated from fresh, virgin powder (build 1) show a single, symmetrical melting endotherm with a peak T_m of 182 °C. However, in parts produced from aged powder a secondary melting peak forms, as an upper-temperature shoulder peak, on the main melting endotherm. The development of this shoulder peak is likely related to the presence of un-molten regions at particle cores within LS parts [38]. Such particles have a higher T_m, and the additional heat provided by the laser is insufficient to fully melt the spherulitic structures present within the particle. The shoulder peak appearing between 190–193 °C supports this theory because this is a similar temperature to the endpoint of melting observed for powder samples recovered from builds 3, 5 and 7 (Table 2).

In Section 3.1.1., it was suggested that polycondensation, and potentially secondary crystallisation, via lamellar thickening, caused T_m to shift to higher temperatures. Un-molten particle cores remaining in the structure of LS parts, indicates the presence of residual crystal fragments. As these fragments only appear in parts produced from aged powder, it would suggest that aged powder contains some particles with thicker crystalline lamellae which are unable to fully melt during the

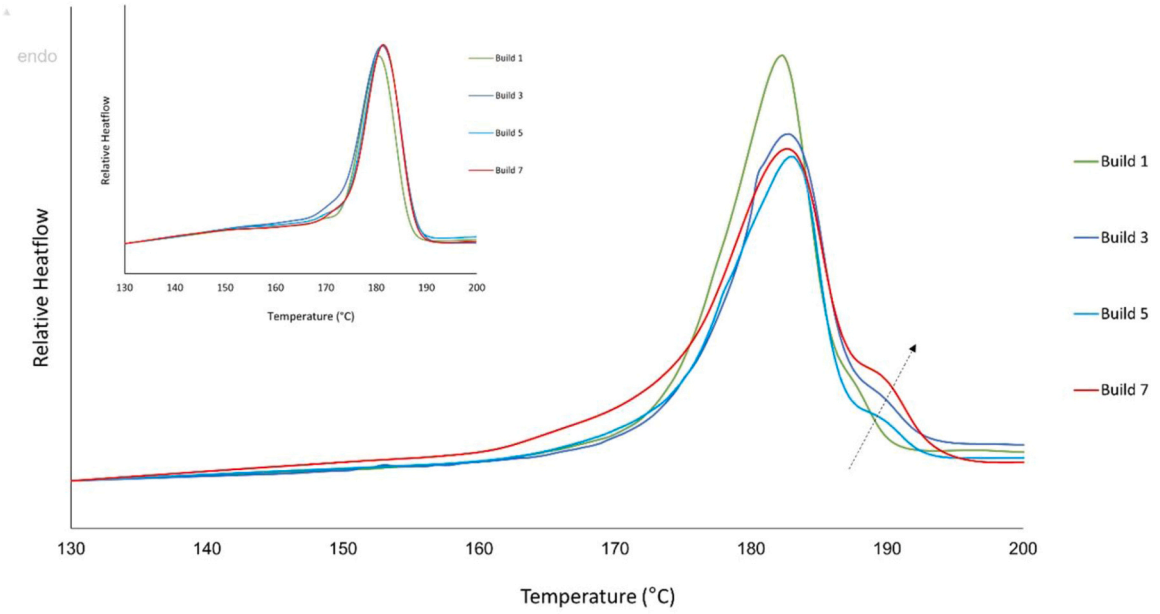

Fig. 8. First heating run recorded on the DSC shows the change in melting behaviour of LS parts as a function of build number. The arrow illustrates the growth of an upper temperature shoulder melting peak which appears in parts fabricated from re-used, aged powder. Insert displays the second heating run, where a single melting endotherm is observed.

sintering process. On the second heating run (Fig. 8, insert), the shoulder peaks disappeared, and all samples displayed a symmetrical melting peak; the previously un-molten particle cores remaining after the build process were fully melted when exposed to higher temperatures within the DSC. This provides further evidence of lamellar thickening because secondary crystallisation is a reversible process. Conversely, although polycondensation is fully reversible under the right conditions, the high temperatures present within a LS build chamber removes the water required for the reverse reaction to occur. Therefore, during LS, increased M_w due to polycondensation is effectively an irreversible change, and the higher T_m structures present in the first heating run would be expected to persist if caused by polycondensation. As such, the thermal behaviour of LS parts emphasises that lamellar thickening is likely occurring (alongside polycondensation), within un-sintered powder during the LS build process.

The presence of unmolten particle cores may lead to hindered particle coalescence, reduced material consolidation, and increased porosity in parts fabricated using re-used powder. Similarly, crystalline fragments remaining due to incomplete melting, could act as nucleation sites during solidification, which would affect the crystallisation kinetics and subsequent crystalline microstructure of LS parts. All of these factors may contribute to the observed reductions in mechanical properties (Section 3.2.2.2), emphasising how deterioration of powder quality can alter the properties and functionality of LS parts. Thermal characterisation of LS parts also provides context to the changes in the melting behaviour of refreshed PA-12 powder (Section 3.1.1). Evidence of incomplete particle melting highlights that 1–4 °C increases in the T_m of PA-12 powder are significant in terms of its suitability for re-use within LS. Within industry, the formation of unmolten regions is a product of ageing which could be overcome by altering certain build parameters. For example, increasing laser power, and decreasing scan speed when printing with a higher proportion of re-used powder, would allow complete melting of all sintered powder particles.

3.2.1.2. Scanning electron microscopy (SEM). The fracture surfaces of tensile samples were analysed to determine whether the deterioration of

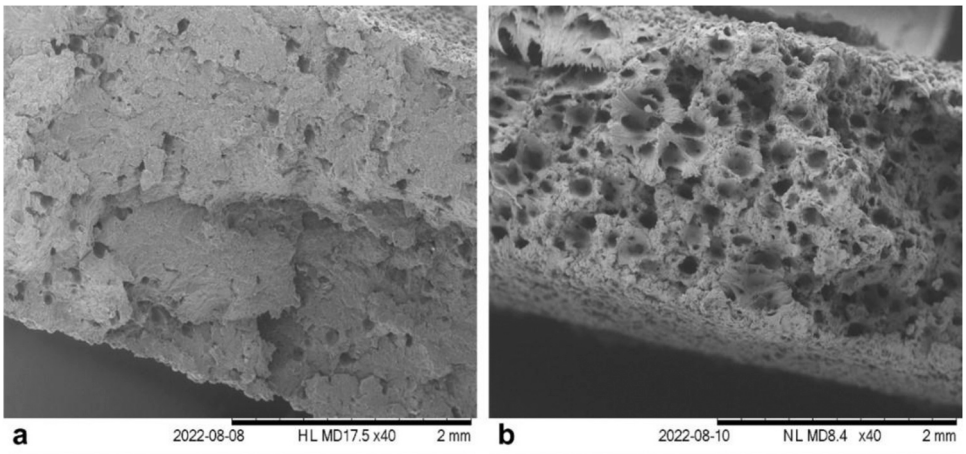

Fig. 9. SEM images, taken using a mix of BSE and SE, displaying the fracture surface of tensile samples, fabricated from a) virgin powder and b) refreshed powder re-used in 3 build cycles.

powder quality causes a change in the microstructure of LS parts. Fig. 9 compares the fracture surfaces of a LS part fabricated using virgin powder (build 1) with a LS samples formed using powder recycled through 3 build cycles (build 4). Build 1 displays some evidence of pores forming but these are randomly situated and low in number. However, build 4 shows a significantly increase in pore size and pore number, with an equal distribution of pores across the surface of the sample.

3.2.1.3. X-ray computed topography (XCT). SEM images only reveal a small cross-section of the fracture surface, so tensile samples were further characterised using X-Ray computed topography (XCT) to quantify the change in porosity with increased build number. Fig. 10 shows that porosity is homogenous throughout all LS parts, and a significant number of pores are present even in parts fabricated from virgin powder. This is due to limitations of the LS process which cause periodic and interlayer porosity, as well as incomplete melting of larger spherulites [8,16,39,58]. With increasing build number, porosity increases and, more specifically, there is a greater number of larger pores.

The increase in porosity with build number is also displayed in Fig. 11a. With repeated powder re-use, the average % porosity of parts increases from 4.4 % in build 1 samples to 10.2 % in samples recovered from build 7. With increased build number, % porosity also displays larger variability, further indicating that used/refreshed powder has a less homogeneous property profile than virgin powder. Across the first five build cycles, the increase in porosity is primarily caused by a 123 % increase in pore size. After build 5 there is then a reduction in pore size which likely explains the subsequent plateau in % porosity. Furthermore, when analysing XCT images it became evident that, independent of build number, porosity is significantly limited when scans are captured near the edge of samples; upon scanning through the thickness of the part, towards the centre, porosity reaches a maximum (Fig. 11b). In this case, it appears that the increased porosity in the centre of parts is caused by a substantial increase in pore number, whilst pore size was generally unaffected. For example, in parts recovered from build 5, XCT scans taken at the edge of samples had an average pore count of 196, whereas the average number of pores in the centre of the part was 1590. This increase in pore number caused the overall porosity to increase from 1.04 % at the part edge to 9.5 % in the centre, as shown in Fig. 11b.

The increase in porosity as a function of build number is likely multifactorial. Ageing processes, such as polycondensation and secondary crystallisation, can cause a rise in T_m and spherulite size, as explained in Section 3.1.1. This could result in the presence of higher melting point particles and an increased number of un-molten spherulite cores (Fig. 8). Furthermore, reduced powder flowability, as discussed in Section 3.1.2, can cause a decrease in coalescence and consolidation of powder particles. Additionally, increased part porosity could be related to the significant particle cracking observed in refreshed powder samples [6], as displayed in Fig. 7.

3.2.2. Mechanical testing of LS parts

3.2.2.1. Effect of build orientation on mechanical properties. Independent of powder re-use, multiple processing parameters such as bed temperature, layer thickness, laser power and laser speed can all effect the mechanical properties of LS parts [59,60]. However, for this study the standard EOS build parameters were locked, so could not be changed for each build. Nonetheless, the orientation of components within the build chamber is also important because parts display anisotropic behaviour, which can significantly affect part density and mechanical properties. Fig. 12 shows the overall change in various mechanical properties as a function of build number and build orientation. The most significant difference, in terms of build orientation, is that samples developed in the ZX (vertical) direction are significantly weaker and are the most brittle (Fig. 12a and 12c). Vertically positioned samples display weaker interlayer bonding, and during a tensile test, the force is applied perpendicular to the print and pore layer direction, which act as crack propagation and failure initiation sites [16,38,61]. Conversely, samples orientated in the horizontal (XY) direction display superior mechanical properties due to a larger and stronger particle bonding area [62,63]. As a result, ZX tensile samples produced during build 2 had a UTS 3.7 MPa lower, and an EAB 14 % less than samples aligned in the XY (horizontal) direction.

3.2.2.2. Effect of build number on mechanical properties. As shown in Fig. 12 there is a reduction in the strength and modulus of all samples, independent of orientation, as a function of build number. This implies that increased material re-use and subsequent ageing of PA-12 powder, has a significant effect on the mechanical properties of fabricated parts in every build orientation. As tensile specimens orientated in the horizontal (XY) direction generally display superior mechanical properties, industrial operators are recommended to print components in the XY orientation. Therefore, in this study, XY tensile specimens were analysed in more detail to show the change in properties as a function of build number.

Fig. 13 shows that, across a total of 7 builds, yield strength and UTS reduce by 24 % and 11 %, respectively, whilst Young's modulus decreased by a relatively modest 7.41 %. The reductions in strength can be explained by the changes in the behaviour of PA-12 powder with increased powder re-use. Increases in T_m, as a result of polycondensation and lamellar thickening, can cause incomplete melting and increase the

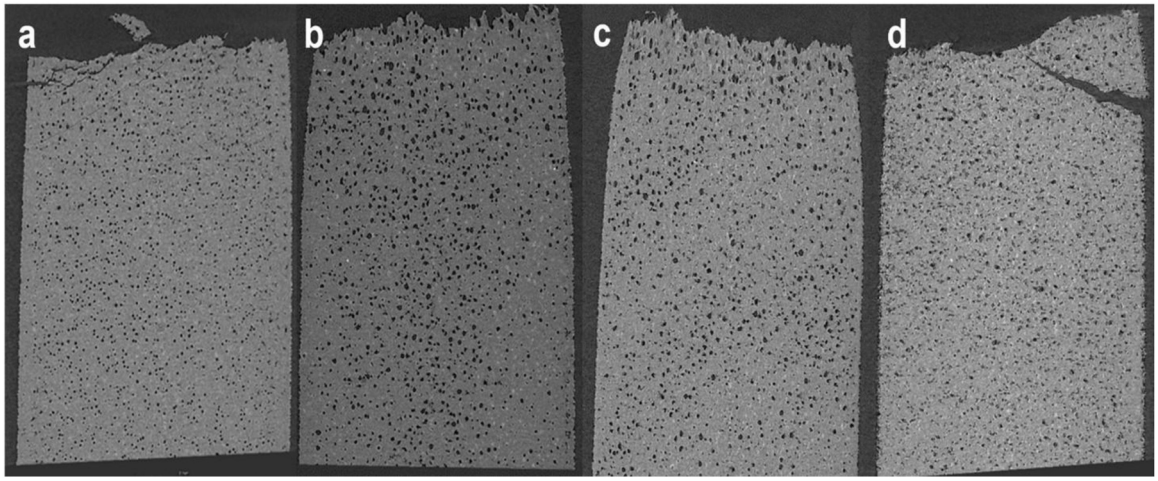

Fig. 10. XCT images taken as transversal cuts throughout the centre of LS tensile specimens recovered from different build cycles: a) 1; b) 4; c) 5 and d) 7.

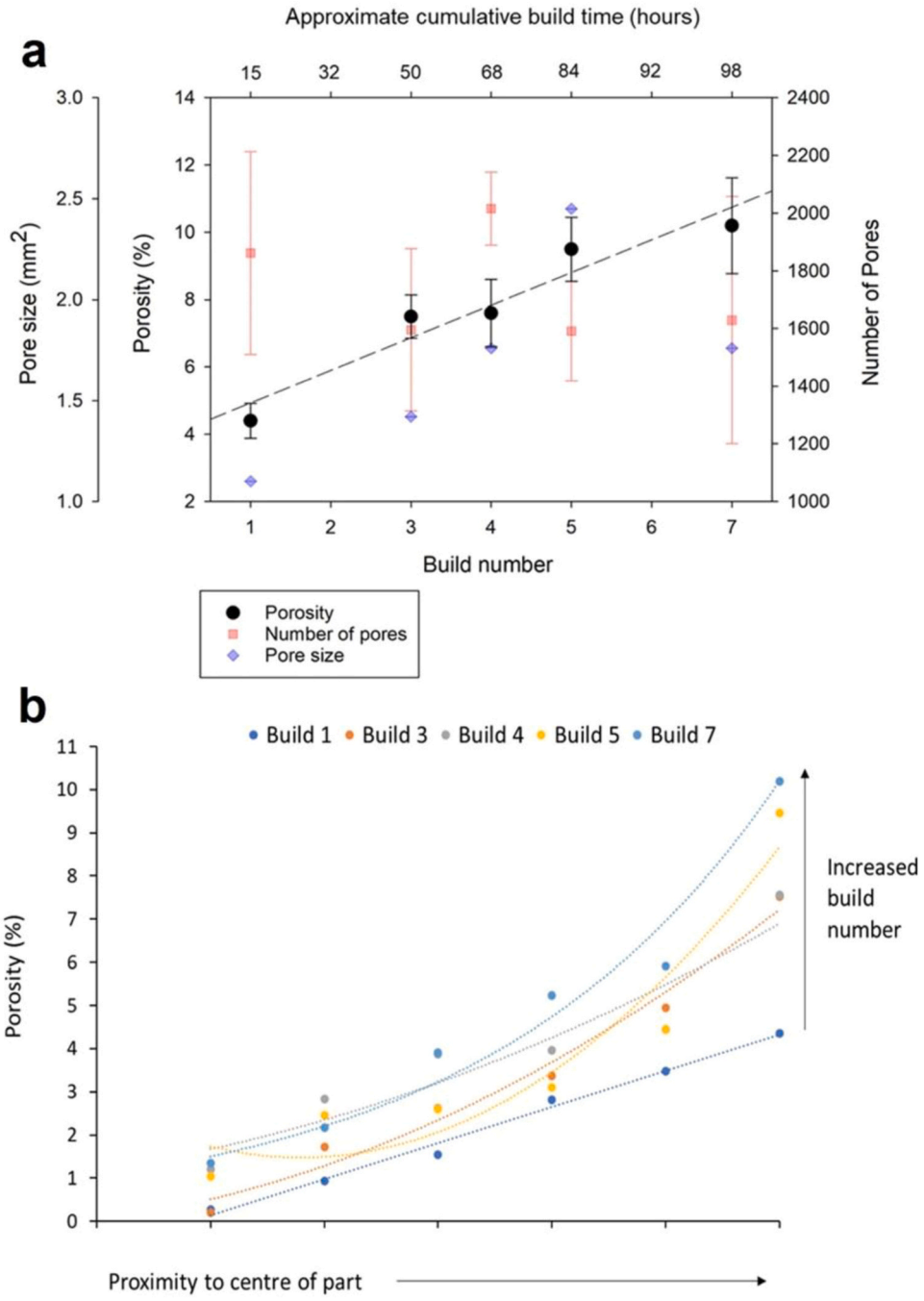

Fig. 11. a) displays the change in average porosity, pore size and pore number as a function of build number and t_c, b) demonstrates how porosity alters throughout the thickness of the 3D tensile specimen. In all cases datapoints are calculated as an average of 5 repeats.

number of nascent particles during sintering. Similarly, polycondensation leads to a higher molecular weight and increased melt viscosity, which may hinder particle coalescence within and between layers [15,24,41]. Reduced particle flowability, as discussed in Section 3.1.2, will likely hinder the spread of powder across the build platform, resulting in voids or agglomeration of powder. As evidenced in Section 3.2.1.3, all of these factors can contribute to increased pore density and an increased number of failure initiation sites, resulting in reductions in UTS and Young's modulus.

However, mechanical testing indicated that, as a function of build number, there was only a minimal change in the elongation at break (EAB) of LS parts. Considering the increase in part porosity, a more significant embrittlement of parts would have been expected. There does appear to be some part embrittlement, however the sample variation within each build is high so the statistical significance of the reductions in EAB is limited. Scattering of elongation at break data has been reported previously by Bourell et al.; they suggested that uneven heating and cooling of the powder bed chamber causes variability in pore distribution and, subsequently, inconsistencies in the ductility of LS samples [39]. Furthermore, due to limitations of the laser sintering technology, it is widely considered that the ductility of LS parts is generally an order of magnitude lower than more traditional manufacturing methods, such as injection moulding [39,64]. As shown in Fig. 10, even virgin parts are relatively porous, consequently, they have a moderately low EAB of 28 %. In parts made from re-used powder, pores remain well distributed throughout the sample, rather than

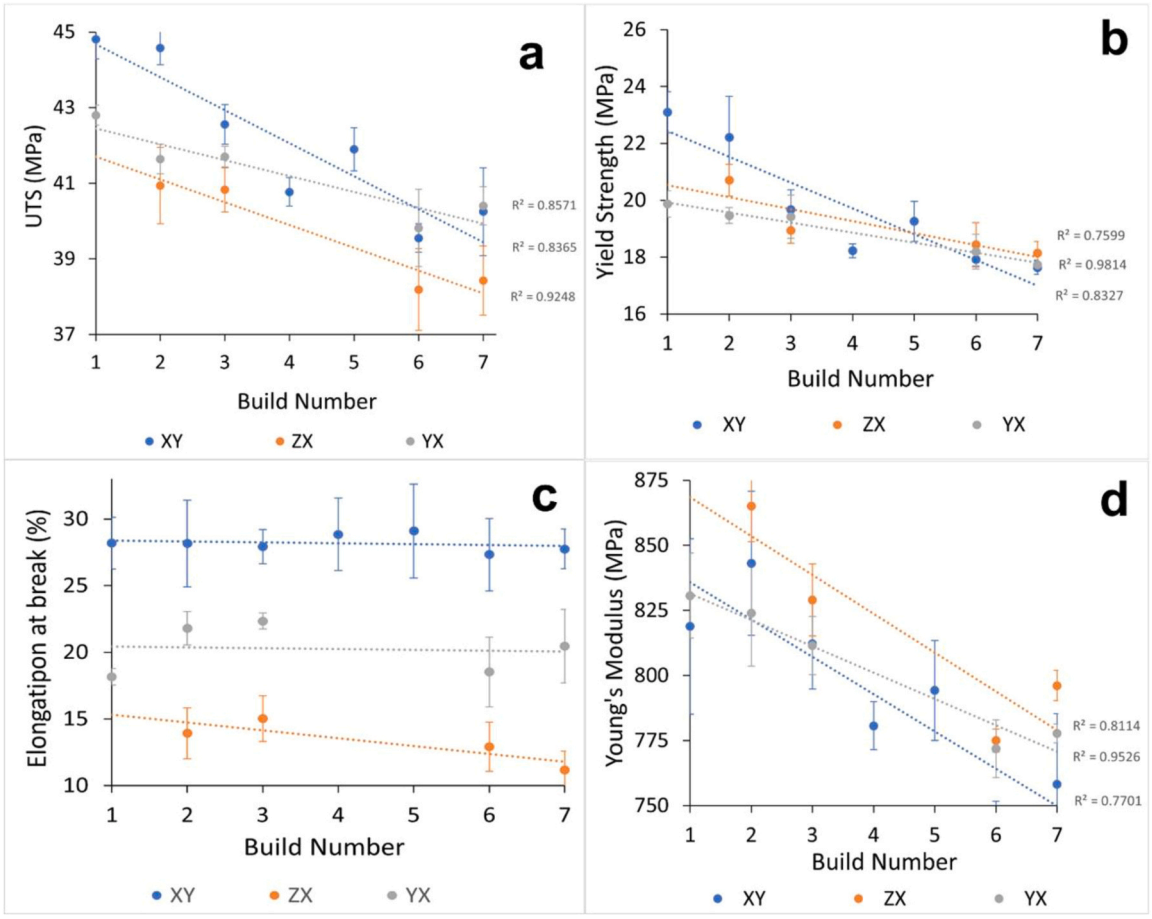

Fig. 12. The change in a) UTS, b) yield strength, c) elongation at break, and d) Young's modulus as a function of build orientation and build number. All datapoints were taken as an average of 5 repeats. Note that some datapoints are missing due to failed builds.

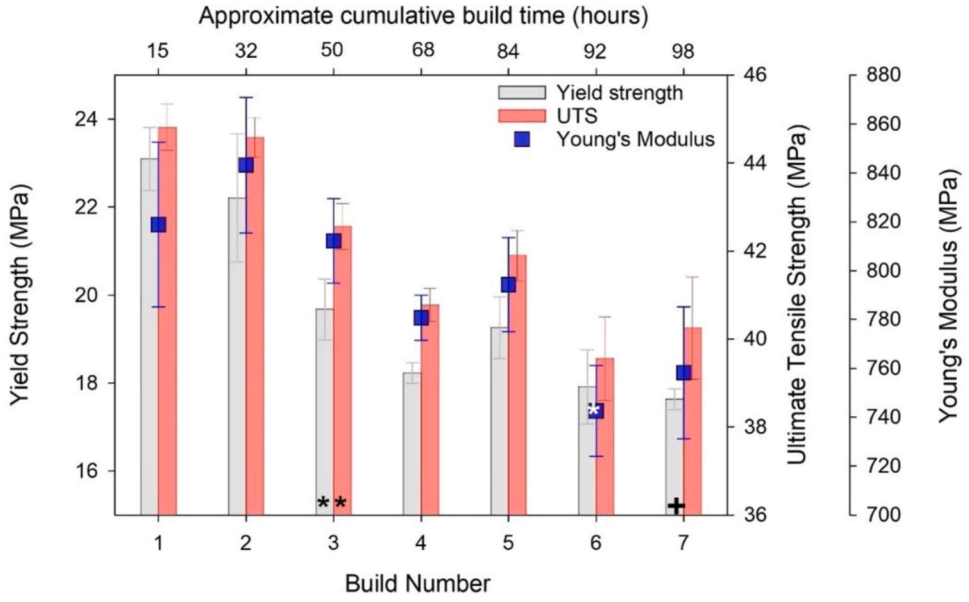

Fig. 13. ANOVA analysis showed that, in the XY build direction, there was a significant change in the averages of Ultimate Tensile Strength, Yield Strength, and Young's Modulus, as a function of build number / t_c. All datapoints are taken as an average of 5 repeats. Post-Hoc T-tests, with the Bonferroni correction, emphasise which build number shows a statistically significant ($P < 0.05$) reduction compared to: * Build 1+ Build 3.

clustering together; this may help prevent weak stress concentrations from forming. Therefore, the 5.8 % increase in porosity across 7 build cycles, although appearing substantial, may not be high enough to induce further embrittlement of an already porous material.

The re-usability of PA-12 powder within LS is a complex problem because, with increased powder re-use, alterations in the property profile of un-sintered powder are multi-factorial and the properties of LS parts are difficult to predict. Statistical analysis of the mechanical performance of LS parts is useful because it emphasises the close relationship between the changes in feedstock powder quality, and subsequent part properties, when re-using PA-12 across multiple build cycles, with a 70:30 refresh ratio. From an industrial standpoint this is useful because it quantifies the stage at which powder re-use has a detrimental effect on part properties. In Section 3.1, Figs. 4 and 5 showed that the most significant increases in T_m and avalanche angle occurred over the first 2 build cycles. Similarly, the largest rise in part porosity occurred between builds 1 to 3 (Fig. 11); consequently, there was a statistically significant reduction in average yield strength and UTS during the 3rd build cycle (Fig. 13). Both powder and part behaviour then display a period of minimal change between build 3 and build 6. Finally, there is a further reduction in the strength of parts fabricated in build 7; directly corresponding to the point at which it was hypothesised that a 70:30 refresh rate was no longer sufficient for maintaining powder quality. As a result, continued powder re-use beyond 7 build cycles would be expected to result in further, more substantial reductions in part strength. Due to the almost parallel changes in the behaviour of powder and sintered parts, the alterations in thermal properties and particle flowability of feedstock powder must explain the observed reduction in part strength. Nonetheless, interpreting the absolute significance of these changes is difficult because the impact is heavily dependent on the industrial application of the component. For example, non-safety critical applications, such as tooling, could withstand some loss of strength and stiffness, whereas in aerospace applications, any reduction in mechanical properties could be critical.

3.3. The relationship between the behaviour of refreshed powder and the properties of final LS parts

The close relationship between the deterioration of powder quality and the mechanical performance of LS parts is further shown in Fig. 14. This emphasises how increases in T_m and avalanche angle, as a result of ageing, are mirrored by a reduction in the UTS of LS parts. Understanding this connection is crucial to improving the recyclability of PA-12 powder. To clarify the sensitivity and effectiveness of the DSC and the RPA for accurately defining whether un-sintered powder is suitable for re-use, it is necessary to quantify the specific relationship between powder and part properties.

A Pearson correlation test can quantify the strength of the relationship between two linearly related variables [65]. Fig. 15 shows that increases in melting temperature, and reductions in flowability, of the supplied powder tend to cause a decrease in the strength of final LS parts. A Pearson correlation test quantified that changes in both T_m and a_a have a statistically significant effect on UTS, as shown by the table in Fig. 15. The relationship between a_a and UTS is stronger, emphasised by the higher Pearson co-efficient and lower p-value, then the same outputs for T_m. The UTS vs a_a correlation is significant to the 0.01 level, whilst UTS vs T_m is still statistically significant, but only to the 0.05 level. Therefore, with increased powder re-use, reduced powder flowability (increased a_a) appears to be the most prominent cause for the decline in mechanical properties of sintered parts. Decreased particle flow can hinder the spread of powder across the build platform, resulting in an uneven, non-homogeneous powder layer; this may prevent full part coalescence and consolidation, leading to regions with significant porosity. Other powder changes, such as increased T_m and a higher number of unmolten particles, will also contribute to reductions in part strength, but the results outlined in this study suggest that decreased powder flow is the most significant factor.

This data suggests that thermal analysis of powder, which is a common characterisation technique within current LS studies, is not necessarily the best indicator of powder reusability. On the other hand,

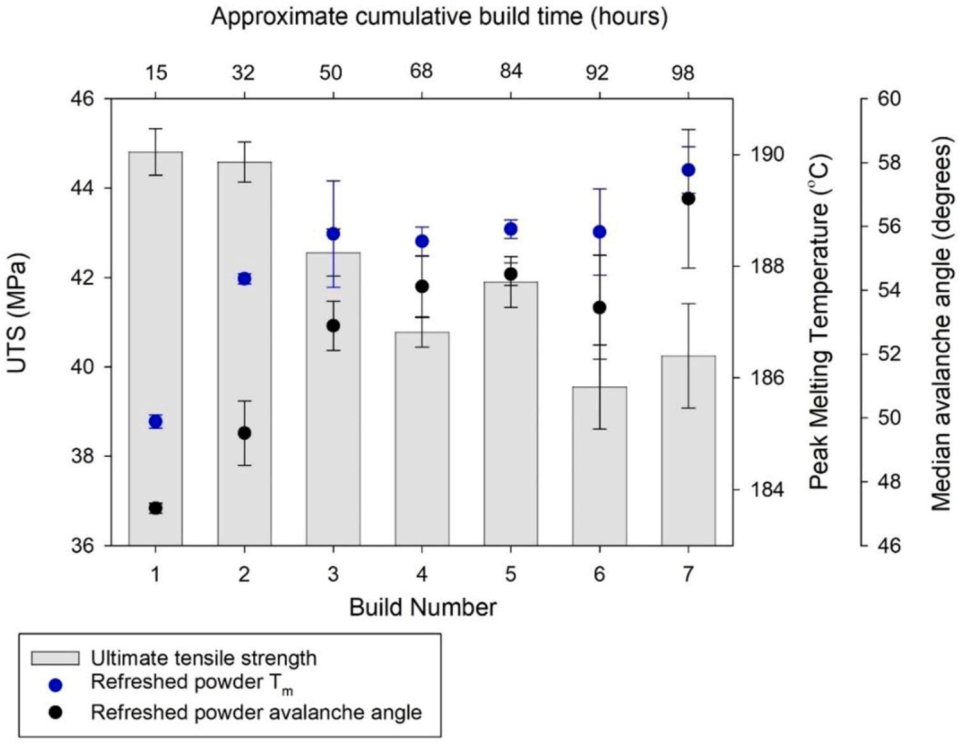

Fig. 14. The relationship between the thermal behaviour and flowability of PA-12 powder, with the mechanical properties of LS parts, as a function of build number and t_c.

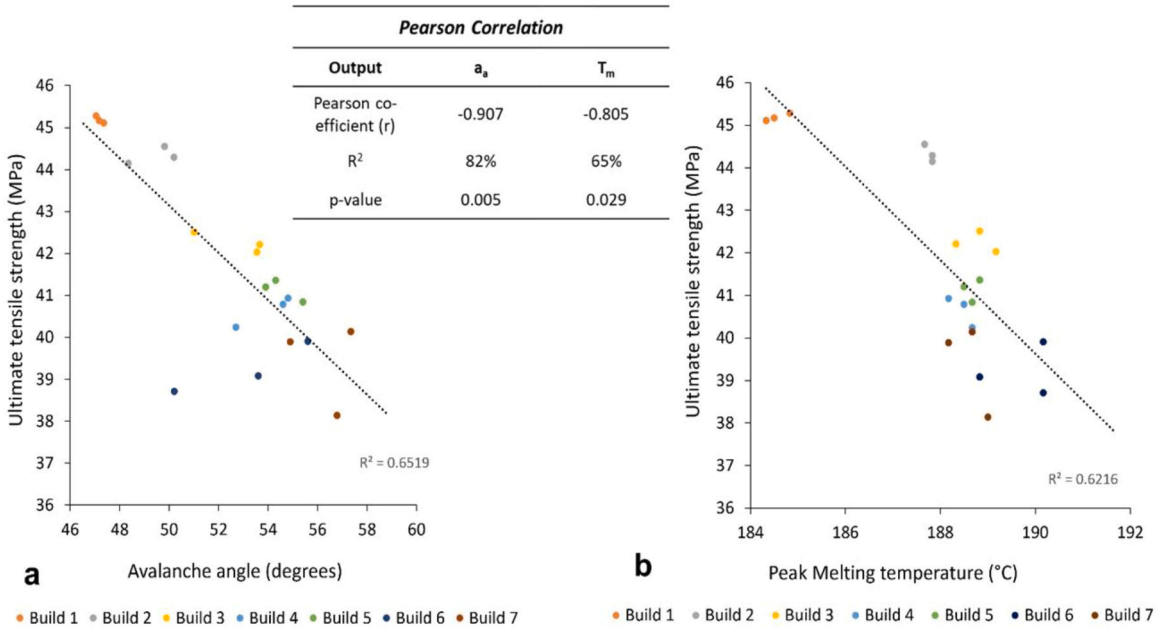

Fig. 15. Displays the negative correlation between UTS and a) increased T_m, and b) increased avalanche angle. A Pearson correlation table quantifies the statistical significance of these relationships.

the RPA is a non-destructive, quick, and energy efficient testing method, which has rarely been used in previous literature, but could be a useful complementary tool for quantifying the quality of PA-12 powder within the LS industry. Therefore, there may be benefits of utilising the RPA alongside other characterisation techniques to optimise and manage the lifecycle of recycled PA-12 powders. As a result, data from this work has contributed to the development of an ASTM work item. This ASTM work item aims to facilitate the development of a standardised set of guidelines that will help define the effectiveness of different characterisation techniques for determining the quality of feedstock powder, and ultimately, its potential for re-use within LS.

Within the LS industry using a 30 or 50 % refresh rate is common practice, but the effectiveness of these refresh ratios for maintaining powder and part quality, over multiple build cycles, has not been explored previously. In a refresh ratio, virgin material is added to dilute the effects of material ageing on the thermal, chemical, and physical properties of feedstock powder; the aim is to ensure that the "refreshed" powder is capable of fabricating high-quality components. However, due to the environmental and economic cost of discarding un-sintered powder, and replacing it with high amounts of virgin material, a compromise is required. Therefore, in this study, a 30 % refresh rate was used to investigate whether powder re-use can be maximised (relative to 50:50), without compromising the quality and functionality of LS parts.

Results showed that powder quality deteriorated as a function of build number, indicating that a 30 % refresh rate may not be sufficient to prevent all the effects of ageing that occur when re-using powder across multiple build cycles; as such, there was a corresponding reduction in the mechanical properties and density of LS parts. Nonetheless, across a total of 7 build cycles, there was only an 11 % reduction in the ultimate tensile strength of sintered parts. This loss of part strength is relatively modest when compared to previous work which employed a similar experimental procedure, but without refreshing the feedstock with any virgin powder [16,24]. Alo et al., stated that parts sintered using virgin powder had a UTS of 40.6 MPa, which is equivalent to the tensile strength measured for build 1 in this study. However, parts printed in build 6 (cumulative build time of ~62 h) displayed a UTS of only 12.8 MPa, which represents a 69 % reduction in UTS [16]. Similarly, Kuehnlein et al., saw a 30 % reduction in UTS after re-using 100 % used powder for 5 build cycles, which correlated to a cumulative build time of only 25 h [24]. Therefore, the results of the current study suggest that, despite alterations in the quality of un-sintered powder, a 70:30 refresh ratio is successful at limiting severe reductions in part strength. This emphasises that a 30 % refresh rate can fabricate LS parts with adequate mechanical properties for most industrial applications, for up to at least 7 build cycles. However, in some application areas, e.g., critical end-use products, an 11 % reduction in strength would be deemed unacceptable. In this scenario, the supply chain could be better organised to re-distribute more severely aged powder to less critical applications, e.g., printing of prototypes. Alternatively, more virgin powder could then be added to the feedstock if necessary. As such, these results appear to show that a 50:50 refresh ratio is only required when manufacturing critical parts where maintaining mechanical performance is vital. Overall, increasing the implementation of a 70:30 refresh rate within industry would reduce the production of LS parts with inadequate mechanical properties, that ultimately have to be discarded; whilst allowing 20 % more un-sintered powder to be re-used every build cycle. This will help decrease the issue of waste, with significant economic and environmental benefits for the LS industry.

4. Conclusion

In this study, using a 70:30 refresh ratio, PA-12 powder was re-used for a total of 7 build cycles, with a cumulative build and cooling time of over 200 h. The relationship between PA-12 powder properties, and the mechanical behaviour of the resulting LS parts, was quantified.

Differential scanning calorimetry (DSC) showed that, with increased build number, there was a rise in the peak melting temperature (T_m) and endpoint of melting (T_me) of used PA-12 powder. These changes in thermal behaviour were attributed to polycondensation and secondary crystallisation. Refreshed powder, with 30 % virgin powder added after each build, displayed an initial shift in T_m to higher temperatures over the first two build cycles, before a plateau. This plateau emphasises how an efficient refresh ratio can help control the thermal properties of feedstock powder. It could be argued that, in order to fully combat polycondensation and prevent increases in T_m, a higher refresh ratio should be applied for the first powder recycle, before reducing the amount of virgin powder added in subsequent builds. However, further work would be required to test this concept of flexible refresh ratios

before implementing this strategy within industry. Particle flowability of refreshed PA-12 powder was analysed using a revolution particle analyser (RPA). With increased re-use there was an increase in avalanche angle, energy, and time, which are all markers of decreased powder flow. The reduction in particle flowability may be explained by a larger number of irregularly shaped particles, the increased presence of fine, satellite particles, and a significant increase in particle cracking within used powder samples.

These observed changes in powder properties affected the property profile of LS parts. Thermal characterisation indicated the presence of un-molten particle cores in parts fabricated from re-used powder, providing evidence of secondary crystallisation occurring within un-sintered powder as a function of powder re-use. Similarly, with increased build number, X-Ray computed topography (XCT) images showed increases in part porosity; this could be related to higher T_m, incomplete particle melting, and reduced flowability of supplied PA-12 powder. Finally, as a function of powder re-use, there was a reduction in ultimate tensile strength (UTS), yield strength, and Young's modulus of LS parts; but part embrittlement was not as significant as expected. A Pearson correlation test quantified that the reduction in powder flow was the most significant cause for the decreased UTS of final parts. However, within certain industrial applications part aesthetics and surface finish may be particularly important, so future work should include an investigation into the effect of extended powder re-use on the aesthetics of the part.

This study provides understanding of the interplay between the quality of feedstock powder and the properties of sintered parts, indicating the benefits of using a 70:30 refresh ratio for the re-use of PA-12 powder in the LS industry. Results imply that the RPA is a useful tool that could be utilised alongside other characterisation techniques to determine powder quality. Overall, data from this study could be utilised to inform improved classification of recycled powder, in order to determine the suitability of powder for re-use in future builds.

Funding

This research did not receive any specific grant from funding agencies in the public, commercial or not-for-profit sectors.

CRediT authorship contribution statement

Jenkins Michael: Writing – review & editing, Supervision, Methodology, Conceptualization. **Cant Edward:** Writing – review & editing, Resources, Methodology, Conceptualization. **Sanders Benjamin:** Writing – original draft, Visualization, Validation, Methodology, Investigation, Formal analysis, Data curation, Conceptualization.

Declaration of Competing Interest

The authors declare that they have no known competing financial interests or personal relationships that could have appeared to influence the work reported in this paper.

Data availability

Data will be made available on request.

Acknowledgements

The authors would like to acknowledge the facilities and technical support of the Manufacturing Technology Centre. The authors would also like to thank Prototal UK Ltd. for providing test specimens and powder samples, and to ASTM for funding the laser sintering build cycles which were completed by Prototal UK Ltd.

References

[1] Goodridge R.D., Ziegelmeier S., editors. Powder bed fusion of polymers 7 2016.
[2] S. Weinmann, C. Bonten, Recycling of PA12 powder for selective laser sintering, AIP Conf. Proc. 2289 (1) (2020) 020056.
[3] K. Dotchev, W. Yusoff, Recycling of polyamide 12 based powders in the laser sintering process, Rapid Prototyp. J. 15 (3) (2009) 192–203.
[4] D.T. Pham, K.D. Dotchev, W.A.Y. Yusoff, Deterioration of polyamide powder properties in the laser sintering process, Proc. Inst. Mech. Eng. Part C: J. Mech. Eng. Sci. 222 (11) (2008) 2163–2176.
[5] R.D. Goodridge, C.J. Tuck, R.J.M. Hague, Laser sintering of polyamides and other polymers, Prog. Mater. Sci. 57 (2) (2012) 229–267.
[6] P.C. Gomes, O.G. Piñeiro, A.C. Alves, O.S. Carneiro, On the reuse of SLS polyamide 12 powder, Materials 15 (16) (2022) 5486.
[7] H.J. O'Connor, A.N. Dickson, D.P. Dowling, Evaluation of the mechanical performance of polymer parts fabricated using a production scale multi jet fusion printing process, Addit. Manuf. 22 (2018) 381–387.
[8] S. Dadbakhsh, L. Verbelen, O. Verkinderen, D. Strobbe, P. Van Puyvelde, J.-P. Kruth, Effect of PA12 powder reuse on coalescence behaviour and microstructure of SLS parts, Eur. Polym. J. 92 (2017) 250–262.
[9] H. Zarringhalam, N. Hopkinson, N.F. Kamperman, J.J. de Vlieger, Effects of processing on microstructure and properties of SLS Nylon 12, Mater. Sci. Eng. A 435-436 (2006) 172–180.
[10] S. Josupeit, H.-J. Schmid, Experimental analysis and modeling of local ageing effects during laser sintering of polyamide 12 in regard to individual thermal histories, J. Appl. Polym. Sci. 134 (42) (2017) 45435.
[11] F. Sillani, R.G. Kleijnen, M. Vetterli, M. Schmid, K. Wegener, Selective laser sintering and multi jet fusion: Process-induced modification of the raw materials and analyses of parts performance, Addit. Manuf. 27 (2019) 32–41.
[12] R.D. Goodridge, R.J.M. Hague, C.J. Tuck, Effect of long-term ageing on the tensile properties of a polyamide 12 laser sintering material, Polym. Test. 29 (4) (2010) 483–493.
[13] C. Yan, Y. Shi, L. Hao, Investigation into the differences in the selective laser sintering between amorphous and semi-crystalline polymers, Int. Polym. Process. 26 (4) (2011) 416–423.
[14] F. Paolucci, M.J.H. van Mook, L.E. Govaert, G.W.M. Peters, Influence of post-condensation on the crystallization kinetics of PA12: from virgin to reused powder, Polymer 175 (2019) 161–170.
[15] F. Yang, T. Jiang, G. Lalier, J. Bartolone, X. Chen, A process control and interlayer heating approach to reuse polyamide 12 powders and create parts with improved mechanical properties in selective laser sintering, J. Manuf. Process. 57 (2020) 828–846.
[16] O.A. Alo, I.O. Otunniyi, D. Mauchline, Correlation of reuse extent with degradation degree of PA 12 powder during laser powder bed fusion and mechanical behavior of sintered parts, Polym. Eng. Sci. 63 (1) (2023) 126–138.
[17] O.A. Alo, I.O. Otunniyi, D. Mauchline, Effects of reuse on morphology, size and shape distributions of PA 12 powder in selective laser sintering and quality of printed parts, J. Polym. Res. 30 (2) (2023) 48.
[18] B. Yao, Z. Li, F. Zhu, Effect of powder recycling on anisotropic tensile properties of selective laser sintered PA2200 polyamide, Eur. Polym. J. 141 (2020) 110093.
[19] S. Rosso, R. Meneghello, L. Biasetto, L. Grigolato, G. Concheri, G. Savio, In-depth comparison of polyamide 12 parts manufactured by multi jet fusion and selective laser sintering, Addit. Manuf. 36 (2020) 101713.
[20] F. Calignano, F. Giuffrida, M. Galati, Effect of the build orientation on the mechanical performance of polymeric parts produced by multi jet fusion and selective laser sintering, J. Manuf. Process. 65 (2021) 271–282.
[21] C. Pandelidi, K.P.M. Lee, M. Kajtaz, Effects of polyamide-11 powder refresh ratios in multi-jet fusion: A comparison of new and used powder, Addit. Manuf. 40 (2021) 101933.
[22] Duddleston L., Puck A., Harris A., Doll N., Osswald T. Differential Scanning Calorimetry (DSC) Quantification of Polyamide 12 (Nylon 12) Degradation during the Selective Laser Sintering (SLS) Process2016.
[23] K. Wudy, D. Drummer, Aging effects of polyamide 12 in selective laser sintering: Molecular weight distribution and thermal properties, Addit. Manuf. 25 (2019) 1–9.
[24] Kuehnlein F., Drummer D., Rietzel D., Seefried A. DEGRADATION BEHAVIOR AND MATERIAL PROPERTIES OF PA12-PLASTIC POWDERS PROCESSED BY POWDER BASED ADDITIVE MANUFACTURING TECHNOLOGIES. 2010;21, No. 1 (1726–9679).
[25] F.M. Mwania, M. Maringa, J.G. van der Walt, A review of the techniques used to characterize laser sintering of polymeric powders for use and re-use in additive manufacturing, Manuf. Rev. 8 (2021) 14.
[26] Wudy K., Drummer D., editors. Aging behavior of polyamide 12: interrelation between bulk characteristics and part properties. Proceedings of the 26th Annual International Solid Freeform Fabrication Symposium, Austin, TX, USA; 2016.
[27] A. Mokrane, Mh Boutaous, S. Xin, Process of selective laser sintering of polymer powders: Modeling, simulation, and validation, Comptes Rendus Mécanique 346 (11) (2018) 1087–1103.
[28] M. Schmid, A. Amado, K. Wegener, Materials perspective of polymers for additive manufacturing with selective laser sintering, J. Mater. Res. 29 (17) (2014) 1824–1832.
[29] J. Riedelbauch, D. Rietzel, G. Witt, Analysis of material aging and the influence on the mechanical properties of polyamide 12 in the Multi Jet Fusion process, Addit. Manuf. 27 (2019) 259–266.

[30] D. Drummer, K. Wudy, M. Drexler, Influence of energy input on degradation behavior of plastic components manufactured by selective laser melting, Phys. Procedia 56 (2014) 176–183.
[31] Kohan M. Nylon Plastics Handbook. Munich (Germany): Hanser 1995.
[32] E.W. Fischer, Effect of annealing and temperature on the morphological structure of polymers, Pure Appl. Chem. 31 (1-2) (1972) 113–132.
[33] M.H.J. Koch, W.H. de Jeu, Crystalline structure and morphology in nylon-12: a small- and wide-angle x-ray scattering study, Macromolecules 36 (5) (2003) 1626–1632.
[34] R.H. Marchessault, Principles of polymer morphology, D. C. Bassett, Cambridge Solid State Series, Cambridge University Press, Cambridge, England, 1981, 250 pp. No price given, J. Polym. Sci.: Polym. Lett. Ed. 20 (5) (1982) 279–280.
[35] B. Sanders, E. Cant, H. Amel, M. Jenkins, The effect of physical aging and degradation on the re-use of polyamide 12 in powder bed fusion, Polymers 14 (13) (2022) 2682.
[36] Duddleston L. Polyamide (Nylon) 12 powder degradation during the selective laser sintering process. MSc, University of Wisconsin. 2015.
[37] Gornet T.J., Davis K.R., Starr T.L., Mulloy K.M., editors. Characterization of Selective Laser Sintering™ Materials to Determine Process Stability 2002.
[38] C. Cai, W.S. Tey, J. Chen, W. Zhu, X. Liu, T. Liu, et al., Comparative study on 3D printing of polyamide 12 by selective laser sintering and multi jet fusion, J. Mater. Process. Technol. 288 (2021) 116882.
[39] D.L. Bourell, T.J. Watt, D.K. Leigh, B. Fulcher, Performance Limitations in Polymer Laser Sintering, Phys. Procedia 56 (2014) 147–156.
[40] D. Drummer, K. Wudy, M. Drexler, Modelling of the aging behavior of polyamide 12 powder during laser melting process, AIP Conf. Proc. 1664 (1) (2015) 160007.
[41] K. Wudy, D. Drummer, F. Kühnlein, M. Drexler, Influence of degradation behavior of polyamide 12 powders in laser sintering process on produced parts, AIP Conf. Proc. 1593 (1) (2014) 691–695.
[42] J. Benz, C. Bonten, Temperature induced ageing of PA12 powder during selective laser sintering process, AIP Conf. Proc. 2055 (1) (2019) 140001.
[43] F. Yang, A. Schnuerch, X. Chen, Quantitative influences of successive reuse on thermal decomposition, molecular evolution, and elemental composition of polyamide 12 residues in selective laser sintering, Int. J. Adv. Manuf. Technol. 115 (9) (2021) 3121–3138.
[44] T. Eggers, H. Rackl, F. von Lacroix, Investigation of the influence of the mixing process on the powder characteristics for cyclic reuse in selective laser sintering, Powders 2 (1) (2023) 32–46.
[45] E.O.S.. Technical Data EOS P396: EOS; [Available from: ⟨https://www.eos.info/en/industrial-3d-printer/plastic/eos-p-396⟩.
[46] T. Kiyotsukuri, T. Hashiba, N. Ozawa, N. Tsutsumi, Thermo-oxidative crosslinking of polyamides by torsional braid analysis, J. Polym. Sci. Part A: Polym. Chem. 26 (12) (1988) 3409–3413.
[47] S. Gogolewski, K. Czerntawska, M. Gastorek, Effect of annealing on thermal properties and crystalline structure of polyamides. Nylon 12 (polylaurolactam), Colloid Polym. Sci. 258 (10) (1980) 1130–1136.
[48] R. Seguela, Critical review of the molecular topology of semicrystalline polymers: the origin and assessment of intercrystalline tie molecules and chain entanglements, J. Polym. Sci. Part B: Polym. Phys. 43 (14) (2005) 1729–1748.
[49] S. Gogolewski, M. Gasiorek, K. Czerniawska, A.J. Pennings, Annealing of melt-crystallized nylon 6, Colloid Polym. Sci. 260 (9) (1982) 859–863.
[50] Amado A., Schmid M., Levy G., Wegener K. Advances in SLS powder characterization. 22nd Annual International Solid Freeform Fabrication Symposium - An Additive Manufacturing Conference, SFF 2011. 2011.
[51] Mercury Scientific. Flowability analysis with the Revolution [Available from: ⟨http://www.mercuryscientific.com/instruments/flowability-analysis-revolution⟩.
[52] Z. Xu, Y. Wang, D. Wu, K.P. Ananth, J. Bai, The process and performance comparison of polyamide 12 manufactured by multi jet fusion and selective laser sintering, J. Manuf. Process. 47 (2019) 419–426.
[53] Ziegelmeier S., Wöllecke F., Tuck C., Goodridge R., editors. Characterizing the bulk & flow behaviour of LS polymer powders. 2013 International Solid Freeform Fabrication Symposium; 2013: University of Texas at Austin.
[54] S.C. Ligon, R. Liska, J. Stampfl, M. Gurr, R. Mülhaupt, Polymers for 3D Printing and Customized Additive Manufacturing, Chem. Rev. 117 (15) (2017) 10212–10290.
[55] C.A. Chatham, T.E. Long, C.B. Williams, A review of the process physics and material screening methods for polymer powder bed fusion additive manufacturing, Prog. Polym. Sci. 93 (2019) 68–95.
[56] M. Schmid, K. Wegener, Additive manufacturing: polymers applicable for laser sintering (LS), Procedia Eng. 149 (2016) 457–464.
[57] P. Chen, H. Wu, W. Zhu, L. Yang, Z. Li, C. Yan, et al., Investigation into the processability, recyclability and crystalline structure of selective laser sintered Polyamide 6 in comparison with Polyamide 12, Polym. Test. 69 (2018) 366–374.
[58] S. Morales-Planas, J. Minguella-Canela, J. Lluma-Fuentes, J.A. Travieso-Rodriguez, A.-A. García-Granada, Multi Jet Fusion PA12 manufacturing parameters for watertightness, strength and tolerances, Materials 11 (8) (2018) 1472.
[59] K. Kozlovsky, J. Schiltz, T. Kreider, M. Kumar, S. Schmid, Mechanical properties of reused nylon feedstock for powder-bed additive manufacturing in orthopedics, Procedia Manuf. 26 (2018) 826–833.
[60] C.S. Abbott, M. Sperry, N.B. Crane, Relationships between porosity and mechanical properties of polyamide 12 parts produced using the laser sintering and multi-jet fusion powder bed fusion processes, J. Manuf. Process. 70 (2021) 55–66.
[61] A.K. Battu, T.R. Pope, T. Varga, J.F. Christ, M.D. Fenn, W.S. Rosenthal, et al., Build orientation dependent microstructure in polymer laser sintering: Relationship to part performance and evolution with aging, Addit. Manuf. 36 (2020) 101464.
[62] L. Feng, Y. Wang, Q. Wei, PA12 powder recycled from SLS for FDM, Polymers (Basel) 11 (4) (2019).
[63] U. Ajoku, N. Saleh, N. Hopkinson, R. Hague, P. Erasenthiran, Investigating mechanical anisotropy and end-of-vector effect in laser-sintered nylon parts, Proc. Inst. Mech. Eng., Part B: J. Eng. Manuf. 220 (7) (2006) 1077–1086.
[64] B. Van Hooreweder, D. Moens, R. Boonen, J.-P. Kruth, P. Sas, On the difference in material structure and fatigue properties of nylon specimens produced by injection molding and selective laser sintering, Polym. Test. 32 (5) (2013) 972–981.
[65] D. Nettleton, Chapter 6 - Selection of Variables and Factor Derivation, in: D. Nettleton (Ed.), Commercial Data Mining, Morgan Kaufmann, Boston, 2014, pp. 79–104.